Mesoscopic heat multiplier and fractionalizer

Florian Stäbler and Eugene Sukhorukov
Département de Physique Théorique, Université de Genève, CH-1211 Genève 4, Switzerland

(Received 11 July 2023; revised 2 November 2023; accepted 17 November 2023; published 6 December 2023)

Local measurements of heat flux in quantum Hall devices can deviate from the expected equilibrium heat flux due to interactions. We present a model of a simple mesoscopic device consisting of an Ohmic reservoir contacted by chiral edge states. In contrast to the well studied heat Coulomb blockade (HCB) effect, we report the opposite phenomenon, an enhancement of the heat flux carried by an edge state in the HCB regime due to an additional contribution of the collective charge mode via the fluctuating potential of the Ohmic contact. We discuss the thermometry of these correlated states and discuss their detectability. The enhancement effect is also reflected in modified correlation functions, which influences the electrical and thermal linear response coefficients in a tunneling probe measurement. On a technical level, we introduce a Langevin formalism that elucidates the role of these extra fluctuations in electrical and thermal transport, both in uniformly heated and Joule heated devices, and argue that our approach has advantages in the latter scenario compared to the standard $P(E)$ theory. We report a violation of the Wiedemann-Franz law, which is modified by the external resistance of the mesoscopic circuit.

DOI: 10.1103/PhysRevB.108.235405

I. INTRODUCTION

The Ohmic contact, a small piece of metal on a highly doped semiconductor region containing a two-dimensional electron gas, is a fundamental component in electron quantum optical experiments. It provides low-resistance contact between edge states and external circuits and control of dephasing [1–9] and energy equilibration [10–12] through strong tunneling. Additionally, it serves as an incoherent source and detector of quasiparticles.

Despite the difficulty of providing a theoretical, microscopic description of an Ohmic contact, progress has been made by considering an effective description in terms of charge and neutral degrees of freedom [13]. The resulting physics is rich and can be attributed to different regimes of macroscopic quantities such as the effective temperature or the charging energy of the contact. Notably, it involves dynamical Coulomb blockade [14,15] in and out of equilibrium, heat Coulomb blockade effect [16,17], Luttinger liquid physics [18–20], charge fractionalization [21,22], and Kondo physics [23–29].

Our recent work focused on using an Ohmic contact as a toy model to investigate the influence of edge reconstruction or disorder on thermal transport in quantum Hall samples [30]. We applied a combination of Langevin equations and scattering theory to a Caldeira-Leggett type system to effectively model dissipation in chiral systems. We proved the quantization of heat for these systems and derived a low-energy theory for the collective degrees of freedom of the edge capturing the universal properties of the edge in the presence of dissipation.

In a subsequent step, we showed how to break the universal quantization of heat flux in nonchiral systems [31], which led to the appearance of a negative heat drag effect due to the presence of extra correlations of the collective charge degree of freedom in the edge. Our main result is that a local measurement of heat can reveal a nontrivial amount of heat current carried by edge states in a globally equilibrium system. This led to the present paper in which we analyze the electrical and thermal properties of these correlated states in a similar device.

In this paper, we present a minimal model of an Ohmic contact, and show that it can host correlated states that emerge due to strong Coulomb interactions similar to the considerations in [21,22]; see Fig. 1. The Ohmic contact is connected to macroscopically large electrodes via n chiral edge states. One additional edge state is prepared such that it forms a loop and is fed back into the Ohmic contact. The anomalous state appears in the looped edge state. The corresponding experimental setup closely resembles the one presented in [16,17]. We show that these correlated states are related to voltage fluctuations of the Ohmic contact, which are in full agreement with $P(E)$ theory [14]; however the role of these extra fluctuations in electrical and thermal transport remains elusive. In the approach presented in this paper we explicitly resolve the temperature dependence of the additional fluctuations, which had to be found with an experimental hypothesis in $P(E)$ theory. We report a multiplication of heat, counterintuitively in the Coulomb blockade regime: a higher than quantum amount of heat carried by the interacting edge states, which poses a paradox of having a hot channel in a globally equilibrium system. The paradox is resolved by coupling this interacting state to another state capacitively or via a quantum point contact (QPC) and explicitly showing energy conservation. We study the linear electrical conductance and thermal tunneling conductance and report a violation of the Wiedemann-Franz law by a number that only depends on the external resistance $R = \frac{R_q}{n}$ of the Ohmic contact $\mathcal{L}_n = 3\frac{2+n}{2+3n}\mathcal{L}_0$, with the resistance quantum $R_q = \frac{h}{e^2}$. Furthermore, we study the Lorenz number

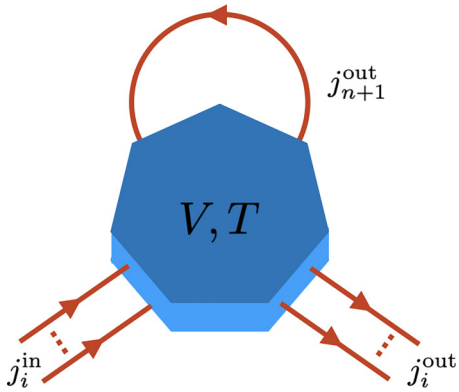

FIG. 1. An Ohmic contact connected to $n \geqslant 1$ external edge states and $m = 1$ looped edge state. This setup can be generalized to multiple loops. A setup like this was already experimentally realized in [16,17]. The loop can be achieved by a quantum point contact (QPC) in the pinch-off regime. As we will show in Sec. IV at finite transmission the QPC can be used to probe the edge state. We consider the Ohmic contact at a uniform temperature T, but experimentally the contact might be heated via Joule heating. This situation can be treated under the assumption of local thermal equilibrium by taking different temperatures in the noise powers of the boundary currents and Langevin sources; see Sec. IV B.

in experimentally more realistic situations and numerically for arbitrary temperatures in equilibrium.

II. MULTIPLICATION OF HEAT CARRIED BY AN EDGE STATE

Let us consider a generalization of the previously proposed model consisting of N incoming and N outgoing edge channels to the Ohmic contact. The bosonic Hamiltonian of this system can be written as

$$\mathcal{H} = \frac{\hbar v_F}{4\pi} \sum_{i=1}^{2N} \int_{-\infty}^{\infty} dx\, [\partial_x \phi_i(x,t)]^2 + \frac{Q^2(t)}{2C}, \tag{1}$$

where $i = 1, \ldots, N$ labels the incoming, and $i = N+1, \ldots, 2N$ the outgoing edge states, and $Q(t) = \sum_{i'} \int_{-\infty}^{0} dx\, \rho_{i'}(x,t) e^{\frac{\varepsilon x}{v_F}}$ is the integral of the charge density $\rho_i(x,t) = \frac{e}{2\pi} \partial_x \phi_i(x,t)$ inside the interaction region $x \in (-\infty, 0]$. The exponentially decaying term arises due to the finite lifetime of excitations ε inside the Ohmic contact. A similar Hamiltonian was used in Refs. [13,32,33]. The Heisenberg equation of motion $\partial_t \phi_i(x,t) = -\frac{i}{\hbar}[\phi_i(x,t), \mathcal{H}]$ can be recast into yet another form,

$$\frac{d}{dt} Q(t) = \sum_{j=1}^{N} \left[j_i^{\text{in}}(t) - j_i^{\text{out}}(t) \right], \tag{2}$$

$$j_i^{\text{out}} = \frac{1}{R_q C} Q(t) + j_i^{\text{c}}(t), \tag{3}$$

where Eq. (2) is Kirchoff's law describing the rate of change of charge on the Ohmic contact in terms of incoming and outgoing boundary currents and Eq. (3) is a Langevin equation that contains a contribution from the collective charge mode via the fluctuating potential $Q(t)/C$ of the Ohmic contact and the neutral thermal current fluctuations $j_n^{\text{c}}(t)$.

Next, consider taking m outgoing states and loop them back onto the Ohmic contact, which reduces the number of unlooped external states to $n = N - m$ incoming and outgoing states, as depicted in Fig. 1 [34]. This can be implemented by an additional constraint on the equation of motion Eqs. (2) and (3) of the form

$$j_k^{\text{in}} = e^{i \frac{\omega L}{v_F}} j_k^{\text{out}}, \quad n < k \leqslant N. \tag{4}$$

Our goal is to compute the heat flux carried by the looped edge states, which is expected to be anomalous, since additionally to the free fermionic neutral excitation carrying a heat flux quantum, we expect the presence of some charge fluctuations adding to this heat flux.

To compute the heat flux carried by any edge state outgoing of the Ohmic contact, we solve Eqs. (2) to (4) and express the outgoing currents in terms of incoming boundary currents and the Langevin sources. For simplicity let us assume that the system is in thermal equilibrium; i.e., the noise power of the incoming boundary current and the noise power of the Langevin sources are equal to an equilibrium noise power at a known temperature $S_{\text{in}} = S_{\text{c}} = S_{\text{eq}}$:

$$S_{\text{eq}}(\omega) = \frac{1}{R_q} \frac{\hbar\omega}{1 - e^{-\beta\hbar\omega}}, \tag{5}$$

where $\beta = \frac{1}{k_B T}$ is the inverse temperature. This constraint will be relaxed in Sec. IV B. Furthermore let us assume that we look at the simple case of one loop $m = 1$ and n external channels and short loops $L = 0$, which corresponds to the experimental situation in [17]. For more general solutions see Appendix A.

To obtain the heat carried by an outgoing edge state we integrate the noise power over all frequencies [35],

$$J = R_q \int_{-\infty}^{\infty} \frac{d\omega}{4\pi} \{ S_i(\omega) - S_i(\omega)|_{T \to 0} \}, \tag{6}$$

where the noise power is defined as

$$S_i(\omega) = 2\pi\delta(\omega + \omega') \left\langle \delta j_i^{\text{out}}(\omega) \delta j_i^{\text{out}}(\omega') \right\rangle \tag{7}$$

and can be found by a Fourier transformation of Eqs. (2) to (4). The noise power is given by

$$S_i(\omega) = S_{\text{eq}}(\omega), \quad 1 < i \leqslant n, \tag{8}$$

$$S_{n+1}(\omega) = \left(1 + \frac{2n}{n^2 + (\omega/\omega_c)^2} \right) S_{\text{eq}}(\omega), \tag{9}$$

where the time constant $\omega_c^{-1} = R_q C = \frac{\pi\hbar}{E_c}$ is related to the charging energy $E_c = \frac{e^2}{2C}$. The expression for the noise power of the external channels is equilibrium as expected from the unitarity of the scattering matrix; however the noise power of the loop acquires an additional contribution due to the charge fluctuations of the Ohmic contact. According to Eq. (6) the heat flux carried by the looped edge state is given by

$$J = \frac{\pi}{12\hbar} k_B^2 T^2 = J_q, \tag{10}$$

for high temperatures compared to the charging energy $\beta E_c \ll 1$, and

$$J = \left(1 + \frac{2}{n} \right) J_q, \tag{11}$$

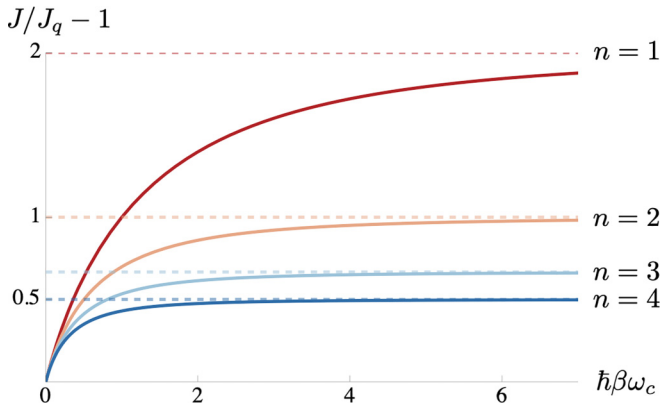

FIG. 2. The excess heat flux in the looped edge state normalized to a quantum $J/J_q - 1$ as a function of the dimensionless inverse temperature $\hbar\beta\omega_c \sim E_c/T$ for $n \in \{1, 2, 3, 4\}$ (solid lines) external edge channels. Note that increasing the number of edge channels decreases the magnitude of the excess heat flux as well as increasing the convergence toward the strongly interacting low-temperature limit (dashed lines).

for low temperatures $\beta E_c \gg 1$. Let us stress again that the anomalous heat flux can be understood as a contribution from the fermionic neutral mode and charge fluctuations created by the Ohmic contact. Solving Eq. (6) numerically allows to explore the intermediate values of J as a function of the channel number n and the dimensionless parameter $\hbar\beta\omega_c \sim E_c/T$. The graph in Fig. 2 shows the dependence of the heat flux for different values of the dimensionless inverse temperature and number of channels.

III. EDGE STATE THERMOMETRY—CAPACITIVE COUPLING

A. Equilibrium operation

In Sec. II we found that a mesoscopic device depicted by Fig. 1 shows a heat flux in the loop that is seemingly higher than the base temperature of the device. In other words, if the device is in global thermal equilibrium, i.e., the temperature of the noise power of the incoming currents and sources are all equal to the base temperature T_0, the heat flux carried by the looped channel is given by Eq. (11) and could also be understood in terms of an effective temperature of the channel $T_{\text{eff}} \sim \sqrt{1 + \frac{2}{n}} T_0$ that is higher than the base temperature.

In a normal resonator a temperature difference would lead to a net energy flux [36]; however here this enhancement is due to charge fluctuations of the Ohmic reservoir. Nevertheless, we need to address this paradox, since it is impossible to extract energy from the system in global equilibrium according to the second law of thermodynamics.

Adding the capacitively coupled channel (see Fig. 3) as a thermometer can be implemented by adding the following equations to Eqs. (2) to (4),

$$\begin{pmatrix} j_{\text{th}}^{\text{out}} \\ j_{n+1}^{\text{in}} \end{pmatrix} = \begin{pmatrix} r_{\text{th}} & t_{\text{th}} \\ t_{\text{th}} & r_{\text{th}} \end{pmatrix} \begin{pmatrix} j_{\text{th}}^{\text{in}} \\ j_{n+1}^{\text{out}} \end{pmatrix}, \tag{12}$$

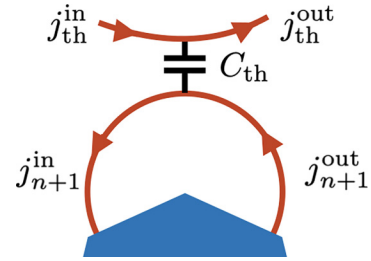

FIG. 3. Capacitive resonator coupling the looped edge state to a free edge state. The thermometer can be operated in equilibrium or with a temperature difference between the edge states.

where the transmission and reflection amplitudes of the thermometer are given by

$$t_{\text{th}} = \frac{1 - 2e^{i\omega t_W} + e^{2i\omega t_W}}{2 - 2e^{i\omega t_W} - i\omega/\omega_{\text{th}}}, \tag{13}$$

$$r_{\text{th}} = \frac{1 - e^{i\omega t_W} + ie^{i\omega t_W}\omega/\omega_{\text{th}}}{2 - 2e^{i\omega t_W} + i\omega/\omega_{\text{th}}}, \tag{14}$$

where $t_W = W/v_F$ is the time of flight through the resonator and $\omega_{\text{th}}^{-1} = R_q C_{\text{th}}$ is the RC time of the capacitive interaction strength between the thermometer and the interacting mode; see Appendix B.

In the next step we compute the heat flux in the outgoing part of the thermometer to check if heat is carried over from the hot channel to the cold channel; using the same protocol described earlier we evaluate Eq. (6). Due to the unitarity of the scattering matrix for the device and thermometer we find the expected result

$$S_{\text{th}}(\omega) = 2\pi\langle \delta j_{\text{th}}^{\text{out}}(\omega)\delta j_{\text{th}}^{\text{out}}(-\omega)\rangle = S_{\text{eq}}, \tag{15}$$

which yields a heat flux quantum according to the equivalent expression to Eq. (6). This resolves the paradox, since no heat can be extracted if the system is in equilibrium and the additional correlations adding to the heat flux exactly cancel in the computation of the outgoing heat flux of the thermometer. This is due to the fact that the capacitive thermometer is invasive. The capacitive coupling is a dynamical, frequency-dependent, coupling even if one considers it only to lowest order in the coupling constant. The incoming state of the thermometer changes the state of the Ohmic contact, and thus the equation of motion of the outgoing thermometer state, such that no heat can be extracted. This is why we consider a truly noninvasive thermometer, modeled as a tunneling junction in Sec. IV.

B. Nonequilibrium operation

Despite the fact that the correlations in the loop remain elusive in an equilibrium setup it is possible to measure signatures of these states in nonequilibrium scenarios. Let us assume a temperature difference across the thermometer. In experiments this would be realized by Joule-heating the Ohmic contact which leads to different effective temperatures for the noise powers of incident current fluctuations T_0, the Langevin sources of the contact T_c, and for generality we will also consider a different temperature of fluctuations incident from the attached thermometer edge state T_{th}. We define the

noise power of incoming current fluctuations to be of equilibrium form but with a different temperature $S_{\rm th}^{\rm in} = S_{\rm eq}(T_{\rm th})$, $S^{\rm in} = S_{\rm eq}(T_0)$, and $S_c = S_{\rm eq}(T_c)$.

A thermometer measurement should be noninvasive, which is why we consider the interacting distance W to be short $\frac{k_B T t_W}{\hbar} \ll 1$. In this case we find the noise power of outgoing current fluctuations of the thermometer $S_{\rm th}(\omega)$ to be

$$S_{\rm th}(\omega) \approx S_{\rm th}^{\rm in}(\omega) + \frac{\omega^2\omega_{\rm th}^2 t_W^4}{\omega^2 + n^2\omega_c^2}\{\omega^2[S_c(\omega) - S_{\rm th}^{\rm in}(\omega)] + n\omega_c^2[(1+n)S_c(\omega) + S^{\rm in}(\omega) - (2+n)S_{\rm th}^{\rm in}(\omega)]\}. \tag{16}$$

Inserting this noise power into the heat integral in Eq. (6) and subtracting the heat flux injected into the thermometer gives the heat flux passed through the thermometer and can be measured downstream of the thermometer edge state. In the noninteracting limit $\omega_c \to 0$ we find

$$\delta J = \frac{k_B^4\pi^3 t_W^4\omega_{\rm th}^2}{30\hbar^3}(T_c^4 - T_{\rm th}^4), \tag{17}$$

and in the strongly interacting limit $\omega_c \to \infty$ we find

$$\delta J = \frac{k_B^4\pi^3 t_W^4\omega_{\rm th}^2}{30n\hbar^3}[T_0^4 + (1+n)T_c^4 - (2+n)T_{\rm th}^4], \tag{18}$$

which shows a dependence on the number of external edge states attached to the Ohmic contact. Note that the correlated state inside the loop can change the (nonuniversal) prefactor of heat flux passed to the thermometer in contrast to the noninteracting case, but not the overall scaling as a function of temperature. Furthermore we note that the outgoing thermometer noise power can be obtained also in other limits or treated nonperturbatively, but this goes beyond the scope of this paper and will be considered elsewhere.

IV. BREAKDOWN OF WIEDEMANN-FRANZ LAW

In the last section we showed that in an equilibrium system it is impossible to see the special features of the looped channel. In nonequilibrium scenarios a capacitive coupling can reveal nontrivial features of these states; however according to Eqs. (13) and (14) this coupling is a dynamical (frequency-dependent) effect.

In this chapter we consider another type of thermometer which consists of a tunneling junction created for example by a QPC. In contrast to the capacitive coupling we consider the transmission amplitudes to be small and frequency independent. In contrast to the capacitive thermometer we expect the looped states to have an anomalous fermionic correlation function which enters the electrical and thermal transport quantities calculated in this chapter. We employ a tunneling Hamiltonian approach and we explicitly consider nonequilibrium situations by studying the linear response current and heat current to a small bias voltage δV and a small temperature difference δT.

A. Lorenz number of tunneling current

Let us assume a coupling of a looped edge state to a free edge state via a quantum point contact (QPC) to leading order of tunneling; see Fig. 4. In this system we also expect no energy transport in equilibrium, but additionally, we report the violation of the Wiedemann-Franz law by a universal number that depends only on the number of external channels, but not on microscopic details of the Ohmic contact, the edge states, or the QPC itself. To do this we employ the tunneling Hamiltonian approach, which allows the computation of both electrical conductance and thermal conductance.

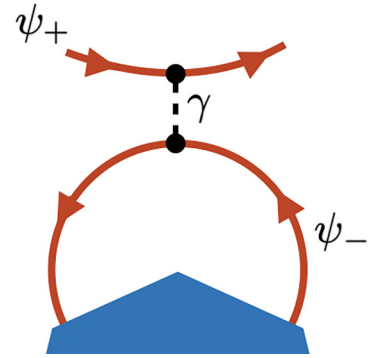

FIG. 4. We describe the QPC using the tunneling Hamiltonian formalism. An electron is created in the "+" edge and annihilated in the "−" edge, or vice versa with a perturbatively small interaction constant γ. The tunneling is switched on adiabatically, which allows us to treat it separately from the Coulomb interactions in the Ohmic contact. We compute the electrical and thermal conductance to leading order in the tunneling constant.

Let us consider the Hamiltonian of the QPC $\mathcal{H} = \sum_{\sigma=\pm}\mathcal{H}_\sigma + \mathcal{H}_T$, which consists of two counterpropagating channels connected by a tunneling term with

$$\mathcal{H}_\sigma = -i\sigma\hbar v_F\int_{-\infty}^{\infty} dx\,\psi_\sigma^\dagger(x,t)\partial_x\psi_\sigma(x,t), \tag{19}$$

$$\mathcal{H}_T = \gamma\psi_+^\dagger(x_0,t)\psi_-(x_0,t) + \text{H.c.} \tag{20}$$

This formalism treats tunneling separately from the interactions at the Ohmic contact, which allows us to impose fermionic boundary conditions for the free edge state ψ_+ and nontrivial interacting boundary conditions due to interactions for ψ_- at the Ohmic contact. For detailed calculations see Appendix C. The average current and average heat flux are defined by the rate of change of charge and energy of the free system, respectively. This gives for the average tunneling current

$$I = \frac{e\gamma^2}{\hbar^2}\int_{-\infty}^{\infty} dt(\langle\psi_+(t)\psi_+^\dagger(0)\rangle\langle\psi_-^\dagger(t)\psi_-(0)\rangle - \langle\psi_+^\dagger(0)\psi_+(t)\rangle\langle\psi_-(0)\psi_-^\dagger(t)\rangle), \tag{21}$$

and for the tunneling heat flux

$$J = \frac{\gamma^2}{i\hbar}\int_{-\infty}^{0} dt(\langle\psi_-^\dagger(0)\psi_-(t)\rangle\langle\dot\psi_+(0)\psi_+^\dagger(t)\rangle - \langle\psi_-(t)\psi_-^\dagger(0)\rangle\langle\psi_+^\dagger(t)\dot\psi_+(0)\rangle), \tag{22}$$

where $\dot\psi(t') = \lim_{t\to t'}\partial_t\psi(t)$.

We evaluate these expressions using the nonequilibrium bosonization technique [37], which allows us to express the vertex operators $\psi_\sigma(t) = \frac{1}{\sqrt{2\pi a}} \exp[i\phi_\sigma(t)]$ in terms of bosonic fields $\phi_\sigma(t)$, which can be found from the currents Eq. (3). Every two-point function can be expressed due to the Gaussian nature of the theory as

$$\langle \psi_\sigma(t)\psi_\sigma^\dagger(t')\rangle = e^{-i\mu_\sigma(t-t')}\mathcal{C}_\sigma(t-t'), \tag{23}$$

$$\langle \psi_\sigma^\dagger(t)\psi_\sigma(t')\rangle = e^{i\mu_\sigma(t-t')}\mathcal{C}_\sigma(t-t'), \tag{24}$$

where the first exponential function is the zero-mode contribution and the phase correlation function $\ln \mathcal{C}_\sigma(t) = \langle[\phi_\sigma(0) - \phi_\sigma(t)]\phi_\sigma(0)\rangle$ is related to the noise power via

$$\ln \mathcal{C}_\sigma(t) = -\frac{2\pi}{e^2}\int \frac{d\omega}{\omega^2} S_\sigma(\omega)(1-e^{-i\omega t}), \tag{25}$$

where $S_+(\omega) = S_{\rm eq}(\omega)$ and $S_-(\omega) = S_{n+1}(\omega)$. The free fermionic phase correlation function is given by the standard expression

$$\mathcal{C}_+(t) = -\frac{i}{2\hbar\beta v_F}\frac{1}{\sinh\left[\frac{\pi}{\hbar\beta}(t-i\eta)\right]}, \tag{26}$$

where the shift of the pole was introduced to find the correct Fourier transformation in terms of the occupation number. For the interacting phase correlation function we find it by relying on a separation of energy scales. The correlation function is altered by the interaction parameter ω_c. For temperatures much larger than the charging energy $\hbar\omega_c \ll k_B T$, we know that our correlation function must have free fermionic character, e.g., due to Eq. (10). For temperatures much smaller than the charging energy, which is in turn much smaller than the UV cutoff, we can find an asymptotic solution in the long-time limit $\omega_c t \gg 1$ of the form

$$\mathcal{C}_-(t) = \frac{\left(\frac{\pi e^{-\gamma_{\rm EM}}}{\omega_c n}\right)^{\frac{2}{n}}}{2v_F}\left(\frac{1}{i\hbar\beta}\frac{1}{\sinh\left[\frac{\pi}{\hbar\beta}(t-t'-i\eta)\right]}\right)^{1+\frac{2}{n}}; \tag{27}$$

see Appendix D.

This allows us to compute Eqs. (22) and (21), which yield very similar expressions, except for the time derivative in the heat flux. Let us start from the average current. Details of the calculations can be found in Appendix E; we will give the results assuming a separation of energy scales given by $k_B T, \hbar t^{-1} \ll \hbar\omega_c \ll \hbar v_F a^{-1}$.

1. Linear conductance

The linear conductance is given by

$$G_n = \frac{e^2}{2\pi\hbar}\frac{\gamma^2}{\hbar^2 v_F^2}\left(\frac{\pi e^{-\gamma_{\rm EM}}}{\hbar\beta\omega_c n}\right)^{\frac{2}{n}}\frac{\sqrt{\pi}\,\Gamma\left(1+\frac{1}{n}\right)}{2\Gamma\left(\frac{3}{2}+\frac{1}{n}\right)}, \tag{28}$$

which in general depends on the number of channels n and reproduces the free fermionic result

$$G_\infty = \frac{e^2}{2\pi\hbar}\frac{\gamma^2}{\hbar^2 v_F^2}. \tag{29}$$

2. Heat flux

It is easy to see that the heat flux is zero for equal temperatures of the two terminals. For a small temperature difference δT (linear response) the heat flux is given by

$$J_n = \frac{4^{\frac{1}{n}}\left[(n-1)\Gamma\left(2+\frac{1}{n}\right)^2 - \Gamma\left(1+\frac{1}{n}\right)\Gamma\left(3+\frac{1}{n}\right)\right]}{n\Gamma\left(4+\frac{2}{n}\right)} \times \frac{\pi k_B \delta T}{\beta\hbar}\left(\frac{\pi e^{-\gamma_{\rm EM}}}{\hbar\beta\omega_c n}\right)^{\frac{2}{n}}\frac{\gamma^2}{\hbar^2 v_F^2}. \tag{30}$$

Especially the noninteracting case gives

$$J_\infty = \frac{\pi k_B \delta T}{6\beta\hbar}\frac{\gamma^2}{\hbar^2 v_F^2}. \tag{31}$$

The Lorenz number for a specific number of channels n is given by

$$\mathcal{L}_n = \frac{J_n k_B \beta}{\delta T G_n} = \frac{2+n}{2+3n}\frac{\pi^2 k_B^2}{e^2} = 3\frac{2+n}{2+3n}\mathcal{L}_\infty. \tag{32}$$

Note that the same result may be obtained by considering transport integrals [38,39].

B. Lorenz number for selective temperature bias

In real experiments, e.g., in the experiments where dynamical Coulomb blockade is studied with a temperature bias [14,16], the Ohmic contact is heated by Joule heating. This may lead to a nonuniform temperature in which the base temperature of the device and the temperature of the sources of the reservoir can be different. In that case the noise power in the loop is not given by Eq. (9), but instead by

$$S_l(\omega) = S_c(\omega) + \frac{n[S_c(\omega) + S_{\rm in}(\omega)]}{n^2 + (\omega/\omega_c)^2}, \tag{33}$$

where the noise power is given by Eq. (5) with the respective temperatures T_c of the Langevin sources and $T_{\rm in}$ for the current fluctuations incident to the device.

In [14], it was stated that after the Joule heating the temperature of the node is different from the temperature of the electromagnetic environment. The best fit to the data was given by the mean temperature of the $(T_{\rm in} + T_c)/2$ with small deviations. We can show with Eq. (33) that this conjecture is valid to leading order in small temperature differences between node and environment and corrections appear in second order of $T_{\rm in} - T_c$. This is a strong advantage of the nonequilibrium bosonization approach [37], which allows us to have a more intuitive physical picture, by describing the voltage fluctuations in terms of boundary currents. This allows us to derive the aforementioned temperature of the voltage fluctuations rigorously.

The nontrivial temperature dependence of the noise power translates directly to the phase correlation function and thus the Lorenz number. Imagine only heating the Ohmic contact and keeping the other channels at base temperature, i.e., $T_{\rm in} = T_+ = T$, where T_+ refers to the temperature of the Fermi distribution of the ψ_+ fermions. This would alter the correlation

function Eq. (27) to

$$\mathcal{C}_-(t) = \frac{\left(\frac{\pi e^{-\gamma_{\mathrm{EM}}}}{\omega_c n}\right)^{\frac{2}{n}}}{2v_F}\left(\frac{k_B T}{i\hbar}\frac{1}{\sinh\left[\frac{\pi k_B T}{\hbar}(t-t'-i\eta)\right]}\right)^{\frac{1}{n}} \times \left(\frac{k_B T_c}{i\hbar}\frac{1}{\sinh\left[\frac{\pi k_B T_c}{\hbar}(t-t'-i\eta)\right]}\right)^{1+\frac{1}{n}}, \tag{34}$$

where we assume $T_c = T + \delta T$ in the linear response regime and repeat the calculations leading to the heat flux Eq. (30). This leads to a modified Lorenz number given by

$$\mathcal{L}_n^{\mathrm{sel.}} = \left(1 + \frac{1}{2+3n}\right)\mathcal{L}_\infty. \tag{35}$$

The maximum Lorenz number is reduced from $\mathcal{L}_1 = \frac{9}{5}$ to $\mathcal{L}_1^{\mathrm{sel.}} = \frac{6}{5}$.

C. Temperature dependence of the Lorenz number

If the separation of energy scales $k_B T, \hbar t^{-1} \ll \hbar\omega_c \ll \hbar v_F a^{-1}$ is not fulfilled, it is possible to study the exact solution for linear conductance and thermal conductance numerically [40]. In the following we plot the Lorenz number for a device with $T_{\mathrm{in}} = T_c$ computed from the numerical solutions of Eqs. (21) and (6) using the exact correlation function, see [14], which after shifting the poles similarly to before gives the following Lorenz number,

$$\frac{\mathcal{L}_n}{\mathcal{L}_\infty} = \frac{\int_0^\infty dx\, \frac{3}{2}[3-\cosh(2x)]\mathrm{sech}^4(x)e^{\Phi(x)}}{\int_0^\infty dx\, \mathrm{sech}^2(x)e^{\Phi(x)}}, \tag{36}$$

with the hyperbolic secant function $\mathrm{sech}(x) = [\cosh(x)]^{-1}$,

$$\Phi(x) = -\frac{2x}{n} + \frac{\pi\left[\cos\left(\frac{n\hbar\beta\omega_c}{2}\right) - e^{-\frac{nx\hbar\beta\omega_c}{\pi}}\right]}{n\sin\left(\frac{n\hbar\beta\omega_c}{2}\right)} - \frac{2\ln(1+e^{-2x})}{n} - \frac{1}{n}\sum_{\sigma=\pm1} H_{\frac{\sigma n\hbar\beta\omega_c}{2\pi}} + e^{-i\frac{\sigma n\hbar\beta\omega_c}{2}+\frac{\sigma nx\hbar\beta\omega_c}{\pi}} B\left(-e^{-2x}; 1+\frac{\sigma n\hbar\beta\omega_c}{2\pi}, 0\right), \tag{37}$$

where H_α is a harmonic number and $B(x;a,b)$ is the incomplete Beta function.

The ratio of the Lorenz number minus 1 is plotted in Fig. 5. Note that a large number of channels suppresses the magnitude of the Lorenz number, i.e., the effect of the voltage fluctuations, but also leads to a faster convergence toward the strongly interacting prediction indicated by the dashed lines upon lowering the temperature. The Lorenz number for arbitrary temperatures can be studied in a more cumbersome but similar way by deriving the equivalent expression of Eq. (36) using Eq. (33).

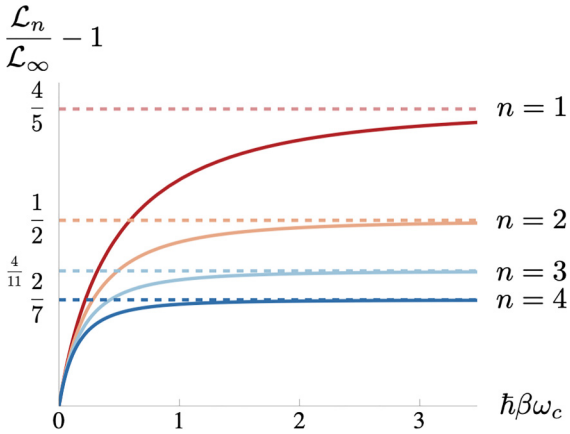

FIG. 5. Numerical values of the Lorenz number for $n \in \{1, 2, 3, 4\}$ (solid lines). The dashed lines indicate the theoretical predictions for the low-temperature, strongly interacting regime.

D. Weak-backscattering limit

If the QPC is operated in the opposite regime of weak tunneling, see Fig. 6, we expect a Lorenz number that is given by the mapping $n \to -(n-1)$; see Appendix C 3. This is in full agreement with the duality in the Luttinger parameter discussed in [14]. The Lorenz number in the weak-backscattering regime is given by

$$\mathcal{L}_n = \frac{3(1-n)}{2-3(1+n)}\mathcal{L}_\infty. \tag{38}$$

E. Additional comments

The Lorenz number presented in this paper was calculated in an experimentally established setup, where the external resistance can only be changed by changing the series

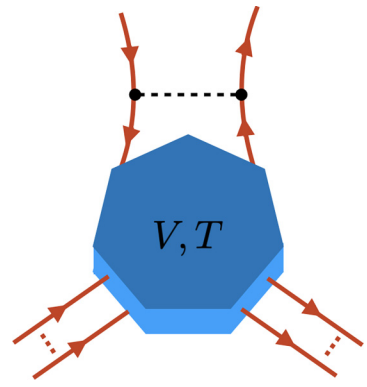

FIG. 6. QPC in the weak-backscattering configuration. The Lorenz number is expected to be dual to the weak-tunneling case.

resistance of the Ohmic contact in discrete steps $R = R_q/n$; however one can also imagine a circuit in series with a macroscopic resistor that can be freely tuned. The computations in this paper do not rely on n being integer, which allows us to immediately generalize our result for an arbitrary series resistance R for the Lorenz number

$$\mathcal{L}_n = 3\frac{2 + R_q/R}{2 + 3R_q/R}\mathcal{L}_\infty. \tag{39}$$

As was shown in [14,18,19,41] there is a direct mapping between an electronic channel in series with a linear resistance and a Tomonaga-Luttinger model (TLL) for an infinitely long 1D system of spinless electrons interacting with a single impurity. The interaction parameter of the TLL is given by

$$K = \left(1 + \frac{R}{R_q}\right)^{-1}, \tag{40}$$

which extends our results directly to the TLL case mentioned above.

A violation of the Wiedemann-Franz law was also reported in interacting Luttinger liquids by [42], but the reported dependence of the prefactor on the interaction parameter is different.

Furthermore we want to note that the Lorenz number given by Eq. (32) for $n \to 1$ appears also in the context of electron tunneling of $\nu = 1/3$ fractional quantum Hall (FQH) quasiparticles; see, e.g., [43]. Our device is similar to the fractionalizer [22] that creates anyonic excitations. Many of the interpretations of the nature of these states can also be applied here.

V. CONCLUSION

In this paper, we provided insights into the previously overlooked heat multiplication effect within Ohmic contacts. The enhancement of locally measured heat flux appears in the Coulomb blockade regime, which at first seems counterintuitive, but is due to the presence of an additional contribution from the collective charge mode via the fluctuating potential $Q(t)/C$ of the Ohmic contact. We used a capacitive resonator and a quantum point contact to perform thermometry on this seemingly hotter edge state and ruled out any paradoxes involving the violation of energy conservation.

One consequence of this is the violation of the tunneling Wiedemann-Franz law leading to a new set of universal Lorenz numbers, the ratio of linear thermal response to voltage response, that depend only on the series resistance R of the circuit. We at first assume a separation of energy scales and study this Lorenz number in the Coulomb blockade regime where the charging energy is much larger than the energy scale set by temperature. We used a combination of Langevin equation and scattering theory to study a uniformly heated and, experimentally more relevant, selectively heated Ohmic contact, leading to a larger than expected Lorenz ratio for both cases. Our approach allows for a more intuitive picture of the role of fluctuations compared to $P(E)$ theory, especially in the context of nonlocal heat transport discussed in [31]. Namely it allows us to derive the experimental hypothesis of the environmental temperature made in [14] rigorously.

We conducted numerical studies to investigate the temperature dependence of the Lorenz number beyond Coulomb blockade regime and discuss how our model can be mapped to continuous resistances, a TLL model, and how it can be applied for fractional fillings, where this approach could be used to probe the edge structure of complicated filling factors. Recently we became aware of Ref. [39] reporting on a similar violation of the Wiedemann-Franz law.

In summary, our findings lay the foundation for further studies on out-of-equilibrium situations involving Ohmic contacts. As an outlook, our results open the way to study this new universality in existing heat Coulomb blockade systems. It can be generalized and adds to the understanding of thermoelectric transport in fractional quantum Hall systems and Kondo circuits.

ACKNOWLEDGMENTS

We would like to thank M. Kiselev for his insight on the hypergeometric function. The authors acknowledge the financial support from the Swiss National Science Foundation.

APPENDIX A: DEPENDENCE ON EXTERNAL RESISTANCE AND NUMBER OF LOOPS

The heat flux transported inside the loop depends on many parameters, namely, the external resistance, i.e., the number of channels attached to the Ohmic contact that do not form a loop, the length of the loop, and the number of loops. The Langevin equations for n external channels and m loops of length L are given by

$$-i\omega Q(\omega) = \sum_{k=1}^{n+m}\left[j_k^{\text{in}}(\omega) - j_k^{\text{out}}(\omega)\right], \tag{A1}$$

$$j_k^{\text{out}}(\omega) = \frac{1}{R_q C}Q(\omega) + j_k^{\text{c}}(\omega), \tag{A2}$$

$$j_l^{\text{in}}(\omega) = e^{i\omega t_{\text{fl}}} j_l^{\text{out}}(\omega), \quad l > n. \tag{A3}$$

1. Noise power for multiple loops of length L with uniform heating

Let us assume equal temperatures for the noise powers of boundary currents and Langevin sources; we find the noise power of one of the looped edge states to be $S_l(\omega) = f(\omega)S_{\text{eq}}(\omega)$, with

$$f(\omega) = 1 - \frac{1}{m + \frac{2mn+n^2+(\omega/\omega_c)^2}{2[m-(m+n)\cos(\omega t_{\text{fl}})+\omega/\omega_c \sin(\omega t_{\text{fl}})]}}, \tag{A4}$$

with $t_{\text{fl}} = L/v_F$. The heat flux carried by the looped edge state can be found by performing the integral in Eq. (6). If we take $L \to \infty$ a separate averaging of $f(\omega)$ over the oscillations shows that $f(\omega) \to 1$. From an experimental point of view the assumption of neglecting potential retardation effect due to a finite length of the loop is justified [17].

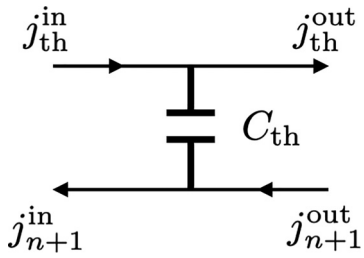

FIG. 7. The labeling of currents of the thermometer.

2. Noise power for short loops with selective heating

In a nonequilibrium situation, where $S_{\rm in} \neq S_{\rm c}$, and under the assumptions of short loops, we find

$$S_l(\omega) = S_{cL}(\omega) + \frac{n[S_c(\omega) + S_{\rm in}(\omega)]}{n^2 + (\omega/\omega_c)^2}, \tag{A5}$$

which reproduces Eq. (9).

APPENDIX B: SCATTERING MATRIX OF THE CAPACITIVE THERMOMETER

The equation of motion for the capacitive thermometer (see Fig. 7) is derived. from a Hamiltonian of two counterpropagating edge states that interact within a region of size W capacitively with coupling strength $C_{\rm th}$,

$$\partial_t \phi_\sigma(x,t) + v_F \partial_x \phi_\sigma(x,t) = -\frac{e}{\hbar C_{\rm th}} Q_{\rm th}\theta(x)\theta(W-x), \tag{B1}$$

where $Q_{\rm th} = \sum_{\sigma'} \int_0^W dx\ \ \rho_{\sigma'}(x)$ is the total charge inside of the interaction region and $\sigma = \pm$ encodes the chirality of the edge states.

The solution of the equations of motion for $0 < x < W$ in terms of bosonic currents is given by

$$j_\sigma(x,\omega) = \tilde{j}_\sigma(\omega) e^{\frac{i\omega\sigma x}{v}} + \frac{1 - e^{\frac{i\omega\sigma x}{v}}}{i\omega/\omega_{\rm th}\sigma} \sum_{\sigma'} \int_0^W dx\ \partial_x j_{\sigma'}(\omega, x), \tag{B2}$$

to which we can assign the boundary currents

$$j_{\rm th}^{\rm in}(\omega) \stackrel{!}{=} j_+(0,\omega), \tag{B3}$$
$$j_{\rm th}^{\rm out}(\omega) \stackrel{!}{=} j_+(W,\omega), \tag{B4}$$
$$j_{\rm n+1}^{\rm in}(\omega) \stackrel{!}{=} -j_-(0,\omega), \tag{B5}$$
$$j_{\rm th}^{\rm out}(\omega) \stackrel{!}{=} -j_-(W,\omega), \tag{B6}$$

which allows us to solve for the S-matrix of the system, which is given by

$$\begin{pmatrix} j_{\rm th}^{\rm out} \\ j_{n+1}^{\rm in} \end{pmatrix} = \begin{pmatrix} r_{\rm th} & t_{\rm th} \\ t_{\rm th} & r_{\rm th} \end{pmatrix} \begin{pmatrix} j_{\rm th}^{\rm in} \\ j_{n+1}^{\rm out} \end{pmatrix}, \tag{B7}$$

where the transmission and reflection amplitudes of the thermometer are given by

$$t_{\rm th} = \frac{1 - 2e^{i\omega t_W} + e^{2i\omega t_W}}{2 - 2e^{i\omega t_W} - i\omega/\omega_{\rm th}}, \tag{B8}$$
$$r_{\rm th} = \frac{1 - e^{i\omega t_W} + ie^{i\omega t_W}\omega/\omega_{\rm th}}{2 - 2e^{i\omega t_W} + i\omega/\omega_{\rm th}}, \tag{B9}$$

where $t_W = W/v_F$ is the time of flight inside the interaction region and $\omega_{\rm th}^{-1} = R_Q C_{\rm th}$ is the RC time of the capacitive interaction strength between the thermometer and the interacting mode.

APPENDIX C: TUNNELING HAMILTONIAN APPROACH

The Hamiltonian of the system is given by

$$\mathcal{H} = \mathcal{H}_+ + \mathcal{H}_- + \mathcal{H}_T, \tag{C1}$$

where

$$\mathcal{H}_\pm = \mp i\hbar v_F \int_{-\infty}^{\infty} dx\, \psi_\pm^\dagger(x,t)\partial_x\psi_\pm(x,t) \tag{C2}$$

and

$$\mathcal{H}_T = \gamma \psi_+^\dagger(x_0,t)\psi_-(x_0,t) + \text{H.c.}, \tag{C3}$$

where we use $\{\psi_+(x,t), \psi_+^\dagger(y,t)\} = \delta(x-y)$.

1. Average heat flux

The heat flux operator is given by

$$\hat{J} = \frac{-i}{\hbar}[\mathcal{H}_+, \mathcal{H}_T] = -\gamma v_F \int_{-\infty}^{\infty} dx \times [\psi_+^\dagger(x,t)\partial_x\psi_+(x,t),\, \psi_+^\dagger(x_0,t)\psi_-(x_0,t) + \text{H.c.}], \tag{C4}$$

where we use the equation of motion and find

$$[\psi_+^\dagger(x,t)\partial_t\psi_+(x,t),\, \psi_+^\dagger(x_0,t)\psi_-(x_0,t)] = -\partial_t\psi_+^\dagger(x_0,t)\psi_-(x_0,t)\delta(x-x_0) \tag{C5}$$

and

$$[\psi_+^\dagger(x,t)\partial_t\psi_+(x,t),\, \psi_-^\dagger(x_0,t)\psi_+(x_0,t)] = -\psi_-^\dagger(x_0,t)\partial_t\psi_+(x_0,t)\delta(x-x_0), \tag{C6}$$

which yields

$$\hat{J} = \gamma[\partial_t\psi_+^\dagger(x_0,t)\psi_-(x_0,t) + \text{H.c.}]. \tag{C7}$$

The average is given by

$$\begin{aligned} J = \langle\hat{J}\rangle &= -\frac{i}{\hbar}\int_{-\infty}^{0} dt\, \langle[J(0), \mathcal{H}(t)]\rangle \\ &= \frac{-i\gamma^2}{\hbar}\int_{-\infty}^{0} dt \\ &\quad \times \langle[\partial_t\psi_+^\dagger(0)\psi_-(0) + \text{H.c.},\, \psi_+^\dagger(t)\psi_-(t) + \text{H.c.}]\rangle \\ &= \frac{-i\gamma^2}{\hbar}\int_{-\infty}^{0} dt\, \langle[\partial_t\psi_+^\dagger(0)\psi_-(0),\, \psi_-^\dagger(t)\psi_+(t)]\rangle \\ &\quad + \langle[\psi_-^\dagger(0)\partial_t\psi_+(0),\, \psi_+^\dagger(t)\psi_-(t)]\rangle \\ &= \frac{-i\gamma^2}{\hbar}\int_{-\infty}^{\infty} dt\, \langle[\partial_t\psi_+^\dagger(0)\psi_-(0),\, \psi_-^\dagger(t)\psi_+(t)]\rangle \\ &= \frac{-i\gamma^2}{\hbar}\int_{-\infty}^{\infty} dt\, \langle\partial_t\psi_+^\dagger(0)\psi_+(t)\rangle\langle\psi_-(0)\psi_-^\dagger(t)\rangle \\ &\quad - \langle\psi_+(t)\partial_t\psi_+^\dagger(0)\rangle\langle\psi_-^\dagger(t)\psi_-(0)\rangle. \end{aligned} \tag{C8}$$

2. Average tunneling current

$$\begin{aligned}\hat{I} &= \frac{-ie}{\hbar}\int_{-\infty}^{\infty} dx[\psi_+^\dagger(x,t)\psi_+(x,t),\mathcal{H}_T]\\ &= \frac{-i\gamma}{\hbar}\int_{-\infty}^{\infty} dx[\psi_+^\dagger(x,t)\psi_+(x,t),\psi_+^\dagger(x_0,t)\psi_-(x_0,t)\\ &\quad + \text{H.c.}]\\ &= \frac{-ie\gamma}{\hbar}\int_{-\infty}^{\infty} dx[\psi_+^\dagger(x,t)\psi_+(x,t),\psi_+^\dagger(x_0,t)\psi_-(x_0,t)]\\ &\quad + [\psi_+^\dagger(x,t)\psi_+(x,t),\psi_-^\dagger(x_0,t)\psi_+(x_0,t)], \end{aligned} \tag{C9}$$

$$\begin{aligned}&[\psi_+^\dagger(x,t)\psi_+(x,t),\psi_+^\dagger(x_0,t)\psi_-(x_0,t)]\\ &\quad = \psi_+^\dagger(x,t)\psi_-(x_0,t)\delta(x-x_0),\end{aligned} \tag{C10}$$

$$\begin{aligned}&[\psi_+^\dagger(x,t)\psi_+(x,t),\psi_-^\dagger(x_0,t)\psi_+(x_0,t)]\\ &\quad = -\psi_+(x,t)\psi_-^\dagger(x_0,t)\delta(x-x_0),\end{aligned} \tag{C11}$$

$$\hat{I} = \frac{-ie\gamma}{\hbar}[\psi_+^\dagger(x_0,t)\psi_-(x_0,t) - \psi_-^\dagger(x_0,t)\psi_+(x_0,t)], \tag{C12}$$

$$\begin{aligned}I = \langle\hat{I}\rangle &= \frac{-i}{\hbar}\int_{-\infty}^{0} dt\langle[I_T(0),\mathcal{H}_T]\rangle\\ &= -\frac{e\gamma^2}{\hbar^2}\int_{-\infty}^{0} dt\langle[\psi_+^\dagger(0)\psi_-(0),\psi_-^\dagger(t)\psi_+(t)]\rangle\\ &\quad - \langle[\psi_-^\dagger(0)\psi_+(0),\psi_+^\dagger(t)\psi_-(t)]\rangle\\ &= -\frac{e\gamma^2}{\hbar^2}\int_{-\infty}^{\infty} dt\langle\psi_+^\dagger(0)\psi_+(t)\rangle\langle\psi_-(0)\psi_-^\dagger(t)\rangle\\ &\quad - \langle\psi_+(t)\psi_+^\dagger(0)\rangle\langle\psi_-^\dagger(t)\psi_-(0)\rangle.\end{aligned} \tag{C13}$$

3. Weak-backscattering limit

In the weak-backscattering limit the correlation functions of the + and − arm cannot be averaged separately. We thus start from the equation for current

$$I = \frac{e\gamma^2}{\hbar^2}\int_{-\infty}^{\infty} dt\langle[\psi_-^\dagger(t)\psi_+(t),\psi_+^\dagger(0)\psi_-(0)]\rangle, \tag{C14}$$

where we resum the exponentials due to the Gaussian nature of the theory. One of the terms in the tunneling current is given by

$$K(t) = \langle e^{-i\phi_-(t)}e^{i\phi_+(t)}e^{-i\phi_+(0)}e^{i\phi_-(0)}\rangle, \tag{C15}$$

$$\begin{aligned}-\ln K(t) &= \int\frac{d\omega}{\omega}\left(1-\frac{2(n+1)}{(n+1)^2+(\omega/\omega_c)^2}\right)\\ &\quad\times\frac{1-e^{-i\omega t}}{1-e^{-\beta\hbar\omega}},\end{aligned} \tag{C16}$$

which implies that the current, but also heat flux and Lorenz number, can be obtained from the weak-backscattering case by the mapping

$$n \to -(n+1), \tag{C17}$$

which is a result of the duality of the weak backscattering and tunneling case.

APPENDIX D: (NON)INTERACTING CORRELATION FUNCTION

1. Free fermionic correlation function

Equation (25) can be manipulated, by rewriting the Bose function as a geometric series, respecting the sign of ω, which gives

$$\begin{aligned}-\ln\mathcal{C}_+(t) &= \frac{2\pi}{e^2}\int\frac{d\omega}{\omega}\frac{1-e^{-i\omega t}}{1-e^{-\beta\hbar\omega}}\\ &= \int_0^\infty\frac{d\omega}{\omega}(1-e^{-i\omega t})e^{-\frac{a\omega}{v_F}}\\ &\quad + \sum_{n=1}^{\infty}\int_0^\infty\frac{d\omega}{\omega}[2-2\cos(\omega t)]e^{-\beta\hbar\omega n}\\ &= \ln\left(\frac{iv_Ft+a}{a}\right) + \sum_{n=1}^{\infty}\ln\left(1+\frac{t^2}{n^2\beta_\pm^2\hbar^2}\right)\\ &= \ln\left[\left(\frac{iv_Ft+a}{a}\right)\prod_{n=1}^{\infty}\left(1+\frac{t^2}{n^2\beta^2\hbar^2}\right)\right]\\ &= \ln\left[\left(\frac{iv_Ft+a}{a}\right)\frac{\hbar\beta}{\pi t}\sinh\left(\frac{\pi t}{\beta\hbar}\right)\right],\end{aligned} \tag{D1}$$

where we introduced the real-space UV cutoff given by a^{-1}, which gives the correlation function

$$\langle\psi_+^\dagger(t)\psi_+(t')\rangle = -\frac{i}{2\pi v_F}\frac{\pi}{\hbar\beta}\frac{e^{i\mu_+(t-t')}}{\sinh\left[\frac{\pi}{\beta\hbar}(t-t'-i\eta)\right]}, \tag{D2}$$

where the shift of the pole is chosen such that we obtain the correct Fermi distribution function if the expression is Fourier transformed, and especially in the zero-temperature limit $\beta\to\infty$ we find

$$\langle\psi_+^\dagger(t)\psi_+(t')\rangle = -\frac{i}{2\pi v_F}\frac{e^{i\mu_+(t-t')}}{t-t'-i\eta}. \tag{D3}$$

The correlation function of the conjugated term can be found according to Eqs. (23) and (24).

2. Interacting case

We would like to find the correlation function respecting the energy following separation of energy scales $k_BT, \hbar t^{-1} \ll \hbar\omega_c \ll \hbar v_F a^{-1}$, where the time t is supposed to be far from the UV regime; i.e., we consider a long-time limit. This gives

$$\begin{aligned}-\ln\mathcal{C}_-(t) &= \int\frac{d\omega}{\omega}\left(1+\frac{2n}{n^2+(\omega/\omega_c)^2}\right)\frac{1-e^{-i\omega t}}{1-e^{-\beta\hbar\omega}}\\ &= -\ln\mathcal{C}_+(t) + \int_{\frac{1}{it}}^{\frac{v_F}{a}}\frac{d\omega}{\omega}\frac{2n}{n^2+(\omega/\omega_c)^2}\\ &\quad + \frac{2}{n}\lim_{t\to\infty}\int_0^{\frac{v_F}{a}}\frac{d\omega}{\omega}(1-e^{-i\omega t}) - \ln\left(i\frac{v_F}{a}t\right)\end{aligned}$$

$$+\frac{2}{n}\sum_{n=1}^{\infty}\int_0^{\infty}\frac{d\omega}{\omega}[2-2\cos(\omega t)]e^{-\beta\hbar\omega n}$$
$$=-\ln\mathcal{C}_+(t)+\frac{2}{n}\left\{\ln\left(in\omega_c t\right)+\gamma_{\mathrm{EM}}+\ln\left[\frac{\hbar\beta}{\pi t}\sinh\left(\frac{\pi t}{\beta\hbar}\right)\right]\right\}, \tag{D4}$$

where $\gamma_{\mathrm{EM}}\approx 0.577\ldots$ is the Euler-Mascheroni constant. First note that the integral can be split into two parts: the free fermionic part and one part that contains the interaction. From now on we only consider the correction. We split the integral into two parts as before. For the temperature-independent part, we cut the integral at $\omega\to\frac{1}{it}$, since the exponential function is fast oscillating for large t. Since the integral is in principle convergent for small frequencies, we have to take into account the possibility to find a constant term that does not vanish in the long-time limit. To do this we also cut the integral at high frequencies only, subtract the logarithmic divergence, which is already accounted for in the long-time limit, and take $t\to\infty$ in what remains. This gives an additional constant factor. The upper limit is given by the UV cutoff. For the temperature-dependent part of the integral, we set $\omega_c\to\infty$, since the charging energy is much larger than the energy scale set by temperature and hence

$$\langle\psi_-^{\dagger}(t)\psi_-(t')\rangle=\underbrace{-\frac{i}{2\pi v_F}\frac{\pi}{\hbar\beta}\frac{e^{i\mu_-(t-t')}}{\sinh\left[\frac{\pi}{\beta\hbar}(t-t'-i\eta)\right]}}_{\text{free fermionic}}\times\left(\frac{\pi}{in\hbar\beta\omega_c e^{\gamma_{\mathrm{EM}}}}\frac{1}{\sinh\left[\frac{\pi}{\beta\hbar}(t-t'-i\eta)\right]}\right)^{\frac{2}{n}}, \tag{D5}$$

and for $\beta\to\infty$

$$\langle\psi_-^{\dagger}(t)\psi_-(t')\rangle=-\frac{i}{2\pi v_F}\frac{e^{i\mu_-(t-t')}}{t-t'-i\eta}\times\left(\frac{1}{in\omega_c e^{\gamma_{\mathrm{EM}}}}\frac{1}{t-t'-i\eta}\right)^{\frac{2}{n}}. \tag{D6}$$

Note that the Euler constant appears only due to how the integral has been regularized. In this case we choose to cut off the integral. Regularization with an exponential decay does not produce this constant as is shown for the free fermionic correlation function, but in any case it remains unphysical and should contribute to the normalization of the correlation function.

APPENDIX E: AVERAGE CURRENT AND AVERAGE HEAT FLUX

1. Average current

The average current is given by Eq. (21), where the correlation functions are given by Eqs. (26) and (27), respectively. This yields the following integral,

$$I=\frac{e\gamma^2}{\hbar^2}\int_{-\infty}^{\infty}dt(\langle\psi_+(t)\psi_+^{\dagger}(0)\rangle\langle\psi_-^{\dagger}(t)\psi_-(0)\rangle-\langle\psi_+^{\dagger}(0)\psi_+(t)\rangle\langle\psi_-(0)\psi_-^{\dagger}(t)\rangle). \tag{E1}$$

At zero temperature, we note that the operator $\psi^{\dagger}$ applied to the ground state creates an electron-like excitation above the Fermi level (with the positive energy), while the operator ψ creates a hole-like one below Fermi level (with the negative energy). One consequence of this is that all singularities in the first term are shifted to the upper half plane of the complex variable t, whereas they are shifted to the lower half plane in the second term. This means only one term contributes depending on the sign of the bias, i.e., depending on whether we close the contour in the upper and lower half plane. At finite temperatures we also have occupied states above the Fermi level, due to thermal activation processes. We thus have to take into account both terms simultaneously,

$$I=-\left(\frac{\pi e^{-\gamma_{\mathrm{EM}}}}{\hbar\beta\omega_c n}\right)^{\frac{2}{n}}\frac{e\gamma^2}{4\pi\hbar^3\beta v_F^2}\int_{-\infty}^{\infty}dt\,e^{i\frac{eV\beta}{\pi}t}\times\sum_{\sigma=\pm1}\frac{\sigma}{\left[-i\sigma\sinh\left(t+i\sigma\frac{\pi\eta}{\hbar\beta}\right)\right]^{2+\frac{2}{n}}}, \tag{E2}$$

where we shift the contour $t\to t+i\sigma\frac{\pi}{2}$ and use that $\sinh(t+i\sigma\frac{\pi}{2})=i\sigma\cosh(t)$ and set $\eta\to 0$. This gives

$$I=-\left(\frac{\pi e^{-\gamma_{\mathrm{EM}}}}{\hbar\beta\omega_c n}\right)^{\frac{2}{n}}\frac{e\gamma^2}{4\pi\hbar^3\beta v_F^2}\int_{-\infty}^{\infty}dt\,e^{i\frac{eV\beta}{\pi}t}\times\sum_{\sigma=\pm1}\frac{\sigma e^{-\frac{eV\beta}{2}}}{\cosh^{2+\frac{2}{n}}(t)}, \tag{E3}$$

where we can perform the sum over σ, which gives

$$I=\left(\frac{\pi e^{-\gamma_{\mathrm{EM}}}}{\hbar\beta\omega_c n}\right)^{\frac{2}{n}}\frac{e\gamma^2}{2\pi\hbar^3\beta v_F^2}\sinh\left(\frac{eV\beta}{2}\right)\times\int_{-\infty}^{\infty}dt\,e^{i\frac{eV\hbar\beta}{\pi}t}\frac{1}{\cosh^{2+\frac{2}{n}}(t)}, \tag{E4}$$

where the last integral can be evaluated by taking $t\to\ln(z)$, and express the result in terms of Gamma functions. We find

$$I=\frac{e\gamma^2}{2\pi\hbar^3\beta v_F^2}\left(\frac{\pi e^{-\gamma_{\mathrm{EM}}}}{\hbar\beta\omega_c n}\right)^{\frac{2}{n}}\sinh\left(\frac{eV\beta}{2}\right)\times\frac{2^{\frac{2+n}{n}}\Gamma\left(1+\frac{1}{n}-\frac{ieV\beta\hbar}{2\pi}\right)\Gamma\left(1+\frac{1}{n}+\frac{ieV\beta\hbar}{2\pi}\right)}{\Gamma\left(2+\frac{2}{n}\right)}, \tag{E5}$$

which gives the linear conductance

$$G_n=\frac{e^2}{2\pi\hbar}\frac{\gamma^2}{\hbar^2 v_F^2}\left(\frac{\pi e^{-\gamma_{\mathrm{EM}}}}{\hbar\beta\omega_c n}\right)^{\frac{2}{n}}\frac{\sqrt{\pi}\Gamma\left(1+\frac{1}{n}\right)}{2\Gamma\left(\frac{3}{2}+\frac{1}{n}\right)}, \tag{E6}$$

which reproduces the free fermionic result

$$G_\infty=\frac{e^2}{2\pi\hbar}\frac{\gamma^2}{\hbar^2 v_F^2}. \tag{E7}$$

2. Average heat flux

The average heat flux is given by a similar expression,

$$J = \frac{-i\gamma^2}{\hbar}\int_{-\infty}^{\infty} dt\,\langle\dot{\psi}_+^\dagger(0)\psi_+(t)\rangle\langle\psi_-(0)\psi_-^\dagger(t)\rangle - \langle\psi_+(t)\dot{\psi}_+^\dagger(0)\rangle\langle\psi_-^\dagger(t)\psi_-(0)\rangle, \tag{E8}$$

in which the correlation functions depend on different temperatures and $\dot{\psi}(t) = \lim_{t'\to t}\partial_{t'}\psi(t')$. For equal temperatures the expression vanishes as expected from the second law of thermodynamics. We assume the temperature difference is small and expand in small δT, which gives the following heat flux,

$$J = -\frac{i}{16n}\frac{k_B\delta T}{\beta\hbar}\left(\frac{\pi e^{-\gamma_{\rm EM}}}{\hbar\beta\omega_c n}\right)^{\frac{2}{n}}\frac{\gamma^2}{\hbar^2 v_F^2}\int_{-\infty}^{\infty} dt\sum_{\sigma=\pm1}(\sigma i)^{\frac{2}{n}}\frac{2t\left[1-n+\cosh\left(2t+\frac{2\pi i\sigma\eta}{\beta\hbar}\right)\right]-(2-n)\sinh\left(2t+\frac{2\pi i\sigma\eta}{\beta\hbar}\right)}{\sigma\sinh^4\left(t+\frac{\pi i\sigma\eta}{\beta\hbar}\right)\sinh^{\frac{2}{n}}\left(t+\frac{\pi i\sigma\eta}{\beta\hbar}\right)}, \tag{E9}$$

where we again shift the poles up and down similarly to before and take $\eta\to 0$, which gives

$$\begin{aligned} J_n &= \frac{1}{8n}\frac{\pi k_B\delta T}{\beta\hbar}\left(\frac{\pi e^{-\gamma_{\rm EM}}}{\hbar\beta\omega_c n}\right)^{\frac{2}{n}}\frac{\gamma^2}{\hbar^2 v_F^2}\int_{-\infty}^{\infty} dt\,\frac{1-n-\cosh(2t)}{\cosh^{4+\frac{2}{n}}(t)} \\ &= \frac{\pi k_B\delta T}{\beta\hbar}\left(\frac{\pi e^{-\gamma_{\rm EM}}}{\hbar\beta\omega_c n}\right)^{\frac{2}{n}}\frac{\gamma^2}{\hbar^2 v_F^2}\frac{4^{\frac{1}{n}}\left[(n-1)\Gamma\left(2+\frac{1}{n}\right)^2-\Gamma\left(1+\frac{1}{n}\right)\Gamma\left(3+\frac{1}{n}\right)\right]}{n\Gamma\left(4+\frac{2}{n}\right)}, \end{aligned} \tag{E10}$$

which can be evaluated as before by the transformation $t\to\ln(z)$. Especially the noninteracting case gives

$$J_\infty = \frac{\pi k_B\delta T}{6\beta\hbar}\frac{\gamma^2}{\hbar^2 v_F^2}. \tag{E11}$$

The Lorenz number for a specific number of channels n is given by

$$\mathcal{L}_n = \frac{J_n k_B\beta}{\delta T G_n} = \frac{\left[(n-1)\Gamma\left(2+\frac{1}{n}\right)^2-\Gamma\left(1+\frac{1}{n}\right)\Gamma\left(3+\frac{1}{n}\right)\right]\Gamma\left(\frac{3}{2}+\frac{1}{n}\right)}{n\Gamma\left(4+\frac{2}{n}\right)\Gamma\left(1+\frac{1}{n}\right)}\frac{2^{2+\frac{2}{n}}\pi^{\frac{3}{2}}k_B^2}{e^2} = \frac{2+n}{2+3n}\frac{\pi^2 k_B^2}{e^2} = 3\frac{2+n}{2+3n}\mathcal{L}_\infty. \tag{E12}$$

[1] I. Neder, F. Marquardt, M. Heiblum, D. Mahalu, and V. Umansky, Nat. Phys. **3**, 534 (2007).

[2] P. Roulleau, F. Portier, P. Roche, A. Cavanna, G. Faini, U. Gennser, and D. Mailly, Phys. Rev. Lett. **102**, 236802 (2009).

[3] P. Roulleau, F. Portier, D. C. Glattli, P. Roche, A. Cavanna, G. Faini, U. Gennser, and D. Mailly, Phys. Rev. Lett. **100**, 126802 (2008).

[4] P.-A. Huynh, F. Portier, H. le Sueur, G. Faini, U. Gennser, D. Mailly, F. Pierre, W. Wegscheider, and P. Roche, Phys. Rev. Lett. **108**, 256802 (2012).

[5] E. Bieri, M. Weiss, O. Göktas, M. Hauser, C. Schönenberger, and S. Oberholzer, Phys. Rev. B **79**, 245324 (2009).

[6] L. V. Litvin, A. Helzel, H.-P. Tranitz, W. Wegscheider, and C. Strunk, Phys. Rev. B **78**, 075303 (2008).

[7] L. V. Litvin, H.-P. Tranitz, W. Wegscheider, and C. Strunk, Phys. Rev. B **75**, 033315 (2007).

[8] A. Helzel, L. V. Litvin, I. P. Levkivskyi, E. V. Sukhorukov, W. Wegscheider, and C. Strunk, Phys. Rev. B **91**, 245419 (2015).

[9] I. Neder, M. Heiblum, Y. Levinson, D. Mahalu, and V. Umansky, Phys. Rev. Lett. **96**, 016804 (2006).

[10] C. Altimiras, H. le Sueur, U. Gennser, A. Cavanna, D. Mailly, and F. Pierre, Phys. Rev. Lett. **105**, 226804 (2010).

[11] C. Altimiras, H. le Sueur, U. Gennser, A. Cavanna, D. Mailly, and F. Pierre, Nat. Phys. **6**, 34 (2010).

[12] H. le Sueur, C. Altimiras, U. Gennser, A. Cavanna, D. Mailly, and F. Pierre, Phys. Rev. Lett. **105**, 056803 (2010).

[13] A. O. Slobodeniuk, I. P. Levkivskyi, and E. V. Sukhorukov, Phys. Rev. B **88**, 165307 (2013).

[14] H. Duprez, F. Pierre, E. Sivre, A. Aassime, F. D. Parmentier, A. Cavanna, A. Ouerghi, U. Gennser, I. Safi, C. Mora, and A. Anthore, Phys. Rev. Res. **3**, 023122 (2021).

[15] C. Altimiras, O. Parlavecchio, P. Joyez, D. Vion, P. Roche, D. Esteve, and F. Portier, Phys. Rev. Lett. **112**, 236803 (2014).

[16] E. Sivre, H. Duprez, A. Anthore, A. Aassime, F. D. Parmentier, A. Cavanna, A. Ouerghi, U. Gennser, and F. Pierre, Nat. Commun. **10**, 5638 (2019).

[17] E. Sivre, A. Anthore, F. D. Parmentier, A. Cavanna, U. Gennser, A. Ouerghi, Y. Jin, and F. Pierre, Nat. Phys. **14**, 145 (2018).

[18] A. Anthore, Z. Iftikhar, E. Boulat, F. D. Parmentier, A. Cavanna, A. Ouerghi, U. Gennser, and F. Pierre, Phys. Rev. X **8**, 031075 (2018).

[19] S. Jezouin, M. Albert, F. D. Parmentier, A. Anthore, U. Gennser, A. Cavanna, I. Safi, and F. Pierre, Nat. Commun. **4**, 1802 (2013).

[20] A. Anthore, D. M. Kennes, E. Boulat, S. Andergassen, F. Pierre, and V. Meden, Eur. Phys. J.: Spec. Top. **229**, 663 (2020).

[21] E. G. Idrisov, I. P. Levkivskyi, and E. V. Sukhorukov, Phys. Rev. B **101**, 245426 (2020).

[22] T. Morel, June-Young M. Lee, H.-S. Sim, and C. Mora, Phys. Rev. B **105**, 075433 (2022).

[23] Z. Iftikhar, S. Jezouin, A. Anthore, U. Gennser, F. D. Parmentier, A. Cavanna, and F. Pierre, Nature (London) **526**, 233 (2015).

[24] Z. Iftikhar, A. Anthore, A. K. Mitchell, F. D. Parmentier, U. Gennser, A. Ouerghi, A. Cavanna, C. Mora, P. Simon, and F. Pierre, Science **360**, 1315 (2018).
[25] H. Kamata, N. Kumada, M. Hashisaka, K. Muraki, and T. Fujisawa, Nat. Nanotechnol. **9**, 177 (2014).
[26] E. Berg, Y. Oreg, E.-A. Kim, and F. von Oppen, Phys. Rev. Lett. **102**, 236402 (2009).
[27] B. Béri, Phys. Rev. Lett. **119**, 027701 (2017).
[28] L. A. Landau, E. Cornfeld, and E. Sela, Phys. Rev. Lett. **120**, 186801 (2018).
[29] H. Inoue, A. Grivnin, N. Ofek, I. Neder, M. Heiblum, V. Umansky, and D. Mahalu, Phys. Rev. Lett. **112**, 166801 (2014).
[30] F. Stäbler and E. Sukhorukov, Phys. Rev. B **105**, 235417 (2022).
[31] F. Stäbler and E. Sukhorukov, Phys. Rev. B **107**, 045403 (2023).
[32] K. A. Matveev, Phys. Rev. B **51**, 1743 (1995).
[33] A. Furusaki and K. A. Matveev, Phys. Rev. B **52**, 16676 (1995).
[34] These states are referred to as external, since the series resistance of the circuit is given by $R = R_q/n$.
[35] The expression for the heat flux used in this paper is motivated from a continuity equation argument; see [30]. Note that the heat flux can sometimes be defined as the integral of the broadening of the electron distribution function $J = \int d\varepsilon\, \varepsilon[f(\epsilon) - \theta(-\epsilon)]$. Since the dispersion relation of the edge states is linear outside of the Ohmic contact these two definitions are the same; see [44].
[36] E. V. Sukhorukov and V. V. Cheianov, Phys. Rev. Lett. **99**, 156801 (2007).
[37] E. V. Sukhorukov, Physica E **77**, 191 (2016).
[38] D. B. Karki, Phys. Rev. B **102**, 245430 (2020).
[39] M. N. Kiselev, Phys. Rev. B **108**, L081108 (2023).
[40] We assume that the tunneling strength γ is the smallest energy scale. Otherwise other perturbations might become relevant. See the discussion in [42].
[41] I. Safi and H. Saleur, Phys. Rev. Lett. **93**, 126602 (2004).
[42] C. L. Kane and M. P. A. Fisher, Phys. Rev. Lett. **76**, 3192 (1996).
[43] C. Nosiglia, J. Park, B. Rosenow, and Y. Gefen, Phys. Rev. B **98**, 115408 (2018).
[44] I. P. Levkivskyi and E. V. Sukhorukov, Phys. Rev. B **85**, 075309 (2012).